RSC Advances

PAPER

View Article Online
View Journal | View Issue

Cite this: *RSC Adv.*, 2023, **13**, 31602

Pathogen inhibition and indication by gelatin nonwoven mats with incorporation of polyphenol derivatives†

By Meng-Yi Bai, *[ab] Ting-Teng Wang,[a] Xin-An Chen[c] and Chia-Chun Wu[c]

There is a need for non-pharmaceutical intervention methods that can prevent and indicate the risk of airborne disease spread. In this study, we developed a nonwoven mat based on the polyphenol gallic acid, which can inhibit pathogens growth and also indicate pathogen levels in the surrounding environment. Using nuclear magnetic resonance, Fourier-transform infrared spectroscopy, and high-performance liquid chromatography, we characterized this novel gelatin-based nonwoven mat and investigated the mechanism governing its ability to indicate pathogen levels. We demonstrated that the incorporation of gallic acid serves a vital role in indicating the presence of bacteria, causing the nonwoven mat to change in color from white to brown. We have proposed a plausible mechanism for this color change behavior based on a reaction of gallic acid with components excreted by bacteria, including glutamate, valine, and leucine. The concentrations of these components reflect the bacterial counts, enabling a real-time indication of pathogen levels in the surrounding air. In summary, the nonwoven mat presented herein can serve as an excellent antibacterial agent and as an indicator of nearby bacteria for fabricating personal protection equipment like filtration mask.

Received 30th August 2023
Accepted 19th October 2023

DOI: 10.1039/d3ra05905g

rsc.li/rsc-advances

1. Introduction

Over 100 million cases of coronavirus disease 2019 (COVID-19) have been reported since December 2019, resulting in millions of deaths.[1,2] The COVID-19 epidemic had a strong social impact that not only transformed living habits but also strained the global economy and increased the demand for medical resources.[3,4] Because this virus can be transmitted between humans through droplets and contact during the incubation period, thus, preventing the spread of virus is difficult. Moreover, virus mutations lead to the need for continuous improvements in vaccines and medicine.[5] Although isolation practices and medical treatment have reduced the influence of the virus infection, such as COVID-19 epidemic, this situation highlighted the type of crises that can occur when a new disease arises and some people refuse or have concerns about vaccines and medications. Therefore, there is a need and inspiration for us to develop a non-pharmaceutical intervention method that can prevent and indicate the risk of airborne disease spread. In this study, we fabricate a nonwoven mat based on polyphenol derivatives that can both inhibit pathogens and indicate pathogen levels in the surrounding environment. Currently used facial mask materials do not have these two functions, which are believed to be crucial for the post-pandemic era.

In a previous study, we found that a sericin-based wound dressing in which ellagic acid was incorporated into a silk fibroin protein (SFP) nonwoven mat membrane could be used as a wound moisture indicator for wound healing management.[6] Because ellagic acid is a polyphenol, this sericin-based wound dressing exhibited antioxidant and antimicrobial abilities, which are well-known functions of polyphenols.[7,8] In an antimicrobial inhibition zone test, we observed an unexpected result: the inhibition zone surrounding the ellagic-acid-incorporated SFP nonwoven mat, which is typically transparent, took on a dark brown color. This serendipitous finding prompted a question: does the region of dark brown color arise from contact between ellagic acid and bacteria? If so, why does this phenomenon occur? However, to the best of our knowledge, the literature survey contains no discussions on a relevant color change mechanism of ellagic acid due to contact with bacteria in an airborne suspension.

As polyphenols represent a group of compounds with similar chemical structure, we thus did a thorough screen on these

[a]*Graduate Institute of Biomedical Engineering and Biomedical Engineering Program, Graduate Institute of Applied Science and Technology, National Taiwan University of Science and Technology, TR-917, AAEON Building, No. 43, Keelung Rd., Sec. 4, Da'an Dist., Taipei City 10607, Taiwan, Republic of China. E-mail: mybai@mail.ntust.edu.tw*

[b]*Adjunct Appointment to the National Defense Medical Center, Taipei 11490, Taiwan, Republic of China*

[c]*Institute of Prevention Medicine, National Defense Medical Center, Taipei 11490, Taiwan, Republic of China*

† Electronic supplementary information (ESI) available. See DOI: https://doi.org/10.1039/d3ra05905g

polyphenol derivatives. Similar to ellagic acid, gallic acid was found to be a natural polyphenol with numerous therapeutic effects, including antioxidant, antimicrobial, antitumor, and anticancer effects.[9,10] Gallic acid is found throughout the plant kingdom and is largely found in free form or as a derivative in various food sources, such as nuts, tea, grapes, and sumac.[11,12] Other sources include gallnuts, oak bark, honey, assorted berries, pomegranate, mango, and other fruits, vegetables, and beverages. Researchers have used gallic acid to crosslink collagen or gelatin molecules through phenolic hydroxyl groups in order to improve the structural, mechanical, antifungal, and antimicrobial properties of the resulting films.[13–15] Although some studies have reported a color change in gallic acid for use as a food expiration indicator, antibacterial inhibition zone indicator, or ultraviolet (UV) absorber to prevent UV exposure,[16,17] there have been no reports on the use of a color change in gallic acid to detect airborne pathogens or studies on a relevant detection mechanism.

Ideally, in this post-pandemic era, a nonwoven mat material for facial masks would be capable of not only passively intercepting pathogens but also indicating pathogen levels around people and actively destroying pathogens. Toward this aim, we fabricated a gallic-acid-incorporated nonwoven mat composed of biocompatible material that can intercept pathogens based on its porous structure, which arises from entangled electrospun fibers within the nonwoven mat.[18] Because of the high surface area of the fibers, when the nonwoven mat intercepts a pathogen, the gallic acid incorporated within the mat can come into contact with and adsorb the pathogen. In this process, we expect the gallic acid to exhibit a color change upon contact with the pathogen, such as bacterial or virus.

In this study, we successfully developed nonwoven mats that can intercept pathogens and provide color information to indicate pathogen levels, as tested for the bacteria *Streptococcus aureus*, *Escherichia coli* and H1N1 virus. Because of the color change behavior of nonwoven mats against bacteria that was serendipitously observed in this study; therefore, bacterial-associated experiments were used to explore the indicative function and protective effect of nonwoven mats. However, COVID-19 pandemic inspires us that the viruses were another one major pathogen that could result in influenza and epidemics in recent years. In virology, influenza A virus subtype H1N1 (A/H1N1) was a subtype of influenza A virus. Influenza A viruses were further classified as different subtypes according to their surface antigens, hemagglutinin (HA) and neuraminidase (NA). The subtypes that were circulating among humans are predominantly H1N1 currently, but H3N2, and H2N2 was also prevalent in the past.[19] Because currently the COVID-19 test is mainly depending on the tedious polymerase chain reaction (PCR) test, in order to preserve the precious medical test resources for those who is really in need, the possibility of common influenza infection should be ruled out firstly in the clinical treatment process, as people got infection of influenza infection show pretty similar symptoms as those of COVID-19 infection. This led us to probe the antiviral and indicative activity of non-woven mats against H1N1 viruses firstly and also avoid sharing the precious COVID-19 research resource at this emergency moment, as COVID-19-associated test needs to be conducted in higher bio-safety laboratory, like BSL4, which pose unique challenges and technical limitations. Of course, COVID-19-relevant indication and prevention research will be the next prominent target of our study. Herein, we confirmed the color change mechanism of the nonwoven mat for indicating pathogen levels by analyzing the constituents of bacterial culture medium *via* nuclear magnetic resonance (NMR) and high-performance liquid chromatography (HPLC). Our results indicate that the color change of the gallic-acid-incorporated nonwoven mat is strongly associated with excretion of the amino acids glutamate, aspartate, leucine and valine during bacterial metabolism. The concentrations of these amino acids reflect the bacterial count, enabling a real-time indication of the degree of pathogen risk in the surrounding air.

2. Experimental

2.1 Materials

Gelatin (100 g; solid; porcine skin; 48724-100G), polycaprolactone (PCL) (250 g; pellets; average Mn 80 000; 440744-250G), and gallic acid (100 g; powder; 97.50–102.50% (titration); G7384-100G) were purchased from Sigma-Aldrich (St. Louis, MO, USA). Luria-Bertani (LB) agar (250 g; powder; SD7003) and LB broth (250 g; powder; SD7002) were purchased from Bio Basic (Amherst, NY, USA).

2.2 Preparation of GgC and GC nonwoven mats

We fabricated gallic-acid-containing gelatin-based nonwoven mats using a stock solution containing gelatin (G), gallic acid (g), and PCL (C). We applied a single-spinneret electrospinning technique, which involved a high-voltage power supply (205B-20R; Bertan, You-Shang Technical Corp, Kaohsiung City, Taiwan) and syringe pumps (NE-300, Just Infusion, Farmingdale, NY, USA), to produce electrospun GgC or GC nonwoven mats (operating distance: 7 cm, operation voltage: 18 kV).

First, 120 mg of gelatin and 30 mg of PCL were separately weighed in two glass vials and dissolved in 300 μL and 200 μL of formic acid, respectively. Second, 400 μL of 0.88 M gallic acid/ethanol solution was divided equally into the two glass vials and stirred well. Finally, the aforementioned mixtures were fed by a syringe pump and electrospun to generate GgC nonwoven mats.

As a control, we also fabricated GC nonwoven mats using the same protocol described above, except that gallic acid was not included in the electrospinning mixtures.

2.3 Morphology characterization

We investigated the fiber structure of the nonwoven mats by scanning electron microscopy (SEM) (JSM-6500F, JEOL, Japan). We utilized Image J (National Institutes of Health, Maryland, USA) to calculate statistical results from the SEM images.

2.4 Color measurement

Bacterial suspensions of *S. aureus* and *E. coli* were prepared in 5 mL of LB broth (25 mg mL^{-1}) and aerobically cultured at 37 °C

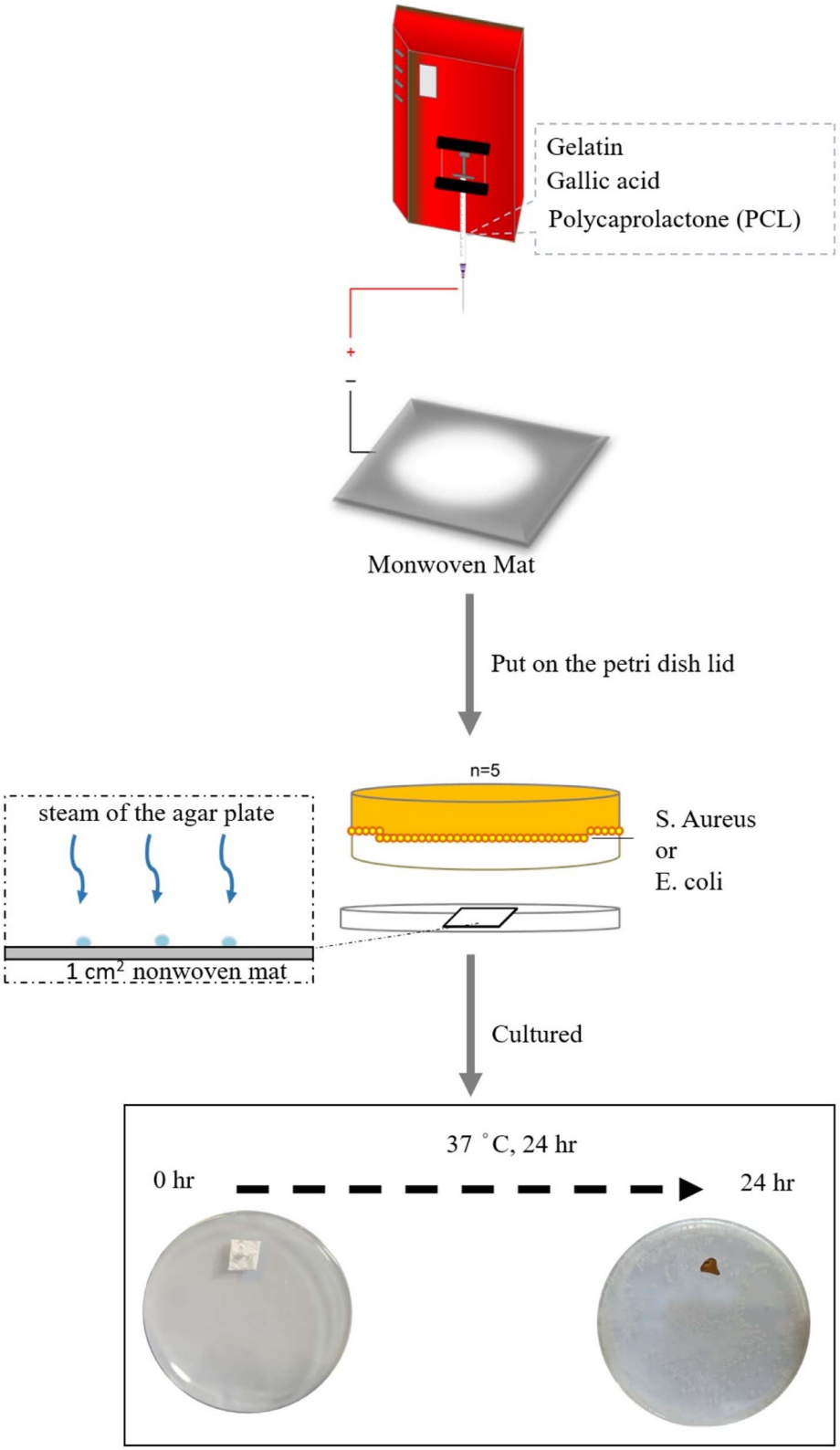

Scheme 1 Schematic illustration of the way for co-culturing GgC nonwoven mat mounted lid placed on the bacterial-streaked agar plate.

for 22 h. We prepared ten-fold serial dilutions of the bacterial suspensions using sterile deionized water and then generated ten different concentrations of bacterial suspensions after ten steps of serial dilution. The diluted solution (150 μL) at each concentration was seeded onto an LB agar plate, and then, a 1 cm^2 GgC nonwoven mat was immobilized on the inner surface

of the Petri dish lid, allowing indirect contact with the streaking bacteria layer on the agar plate. Typically, the GgC nonwoven mat mounted lid was placed on the agar plate, and the agar plate was then positioned upside-down and aerobically cultured at 37 °C for 24 h (as shown Scheme 1). The numbers of colony-forming units (CFU) for each concentration were tallied and calculated. We quantified the color change of the GgC nonwoven mats using the CMYK code at the CMYK tool website. We were able to define the biothreat degree associated with the color change of the mats based on the CFU growth on the agar plate and the CMYK code of the brown color observed on the GgC nonwoven mats.

2.5 Analysis of bacterial excretion

We probed the mechanism by which the mats indicated the pathogen level by analyzing the bacterial excretion. A bacterial suspension (300 μL) was seeded onto an LB agar plate and aerobically cultured at 37 °C for 24 h. When the bacteria grew to colonies, the excreta that could rise as a vapor was emitted from the agar plate. We collected the vapor as a condensed liquid by placing the upside-down Petri dish on dry ice. The condensed liquid was harvested and immediately analyzed by high performance liquid chromatography (HPLC, LC-40D, Shimadzu, Kyoto, Japan) and NMR (Avance III HD-600 MHz, Bruker, Massachusetts, U.S.). Moreover, we identified the functional groups on top of the GgC nonwoven mats using a Fourier-transform infrared spectroscopy (FTIR) instrument (FT/IR-4680, JASCO, Oklahoma City, Oklahoma, USA) equipped with an attenuated total reflection accessory.

2.6 Bactericidal assay

We divided the bacterial suspension into four groups ($n = 4$) to conduct four sets of bactericidal assays with different material treatment, including a positive control (treated with tetracycline), a negative control (no treatment), experimental groups (treated with 10 000 ppm GgC/extract medium or 20 000 ppm GgC/extract medium, respectively). All groups were aerobically cultured at 37 °C for 24 h. We then prepared ten-fold serial dilutions for each group using sterile deionized water. We seeded the ten-fold serial dilution solution (150 μL for each concentration) onto LB agar plates, which were aerobically cultured at 37 °C for 20 h. The amounts of bacteria (CFU mL^{-1}) and sterilization percentage were determined from eqn (1) and (2), respectively. In the time-kill curve assay, viability counts were performed at 0, 1, 5 and 24 h of incubation at 37 °C by plating the ten-fold serial dilution solution of four groups ($n = 5$) onto LB agar plates, which were aerobically cultured at 37 °C for 20 h.

$$\text{CFU mL}^{-1} = \left(\frac{C \times 1000}{150}\right) \times N \quad (1)$$

Eqn (1) gives the amounts of bacteria (CFU mL^{-1}) in the target dilution, where C is the number of colonies tallied in the agar medium and N is the dilution ratio in a ten-fold serial dilution.

$$\text{Sterilization percentage} = \left(\frac{\text{CFU of medium group} - \text{CFU of target group}}{\text{CFU of medium group}}\right) \times 100\% \quad (2)$$

Eqn (2) gives the sterilization percentage of the target group.

2.7 Plaque assay

In plaque therapy assay, the Tamiflu was added to the negative control as an inhibitory medium. Tamiflu (Oseltamivir) was an antiviral medication that was used for the prevention and treatment of influenza caused by influenza A and B viruses in the current clinical practice and treatment. The MDCK cells were seeded in 6 well culture plates (6×10^5 cells per well) at 37 °C for 24 h. H1N1 virus solution was mixed with inhibitory medium (Tamiflu or 1000 ppm nonwoven mat medium solutions) for 1 h, and then the MDCK cells were infected with H1N1 virus solution for 1 h. Afterward, the virus-containing culture medium was removed and the infected cells were washed with PBS. The inhibitory medium (0.5 mL per well) and 1.02% Avicel (3 mL per well) were added and cultured with the infected cells at 37 °C and 5% CO_2. After 3 days, we removed the inhibitory medium and washed the infected cells with PBS. And then, 1% crystal violet (containing 10% paraformaldehyde) was added to each well (0.5 mL per well) for 30 minutes which could stain the infected cells. The numbers of virus potency (PFU mL^{-1}, plaque forming unit) for each group were tallied and calculated.

In plaque neutralization assay, the MDCK cells were seeded in 6 well culture plates (6×10^5 cells per well) at 37 °C for 24 h. H1N1 virus solution was mixed with inhibitory medium (Tamiflu or 40000 ppm nonwoven mat medium solutions) for 1 h, and then the MDCK cells were infected with H1N1 virus solution for 1 h. Afterward, the virus-containing culture medium was removed and the infected cells were washed with PBS. The normal medium (0.5 mL per well) and 1.02% Avicel (3 mL per well) were added and cultured with the infected cells at 37 °C and 5% CO_2. After 3 days, we removed the inhibitory medium and washed the infected cells with PBS. And then, 1% crystal violet (containing 10% paraformaldehyde) was added to each well (0.5 mL per well) for 30 minutes which could stain the infected cells. The numbers of virus potency (PFU mL^{-1}, plaque forming unit) for each group were tallied and calculated.

3. Results and discussion

3.1 Surface morphology of the GgC nonwoven mats

We used gelatin and PCL, which are both biodegradable materials, to prepare the nonwoven mats. Gelatin is a tasteless, colorless biopolymer derived from collagen. Because of its advantages, including its biological origin, biodegradability, and biocompatibility, researchers have utilized gelatin for applications in wound healing and drug delivery.[20,21] However, gelatin has poor mechanical properties and viscosity. For this reason, some researchers have sought to improve its exterior, structure, film formation, and mechanical properties by the

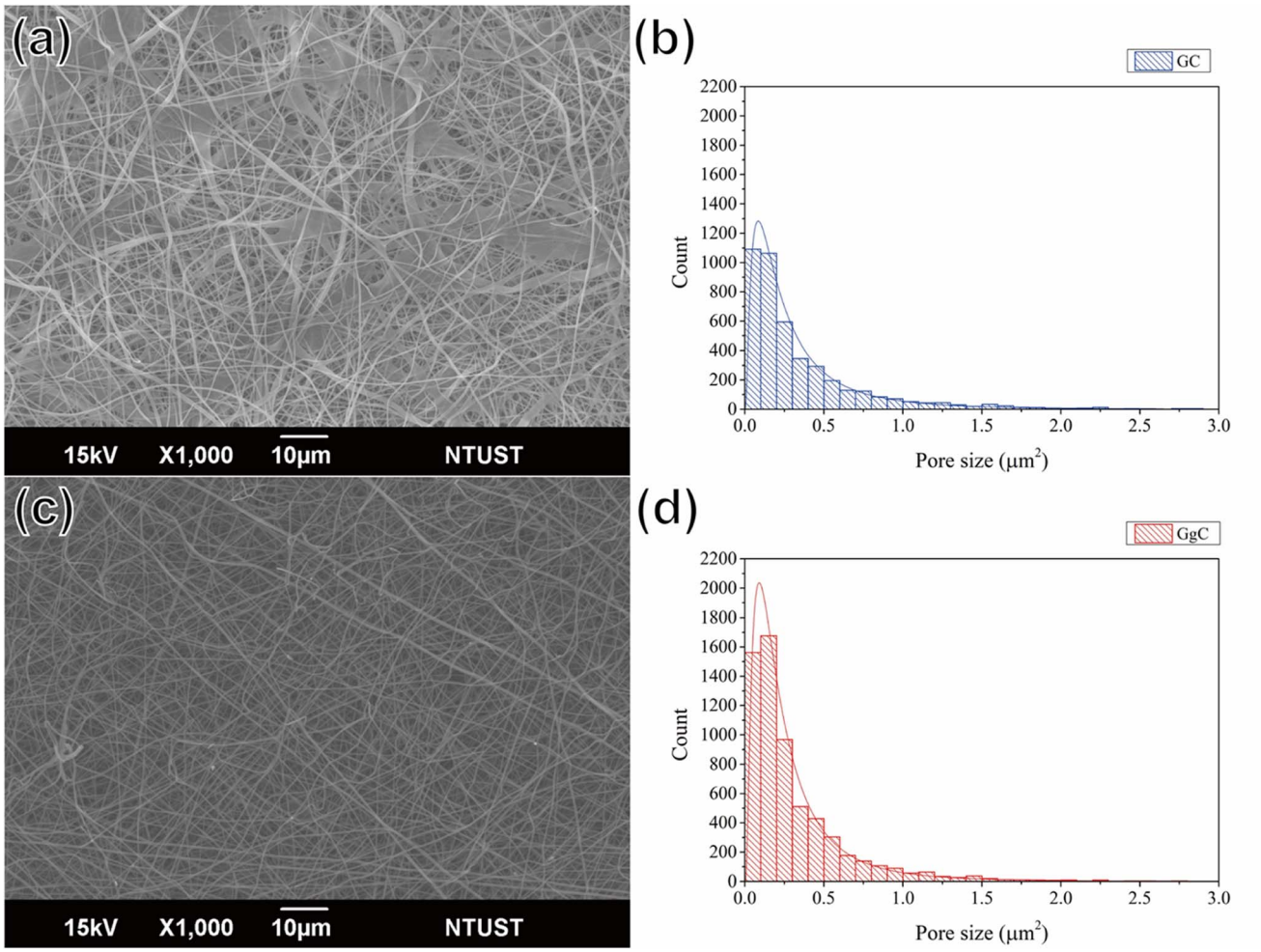

Fig. 1 SEM images of (a) GC and (c) GgC nonwoven mats. Pore size distribution of (b) GC and (d) GgC nonwoven mats.

addition of sodium alginate, ferulate, or PCL.[22] In this work, gelatin and PCL were chosen to mix and spray from an electrospinning system due to their friendly biodegradability to the environment. The resulting mat consists of thick fibers with a porous structure, as shown by the results in Fig. 1(a) and (b) for the GC mat. Fig. 1(c) shows an SEM image of the GgC mat, in which gallic acid was used to crosslink the gelatin *via* hydrogen bonding and to stabilize the fiber structure. We found that the use of gallic acid not only increased the number of pores (size approximately falling in the range of 0–0.4 μm^2), but also increased the porosity from 14.41% to 17.67%, as demonstrated by the image and statistical results shown in Fig. 1(b)–(d). The primary constituted pores (0–0.2 μm^2) of the GgC nonwoven mat are smaller than most bacteria, aerosol and particulate matter; therefore, we expect the pores on the GgC nonwoven mat to intercept typical air pollutants.

3.2 Relationship between nonwoven mat color and pathogen count in the environment

Fig. 2 presents color results for the GgC nonwoven mat upon indirect contact with a known colony of *S. aureus* or *E. coli* grown on the agar plate. To obtain these results, we seeded known amounts of bacteria onto agar plates and placed lids with GgC nonwoven mat mounted inside on the agar plates. The excretion contents from the colonies on the agar plate then rose to fill the confined space inside the plate during the culture process. These excretion contents were able to react with the GgC nonwoven mat mounted on the inner side of the plate cap, causing the color of the mat to change from white to brown.

For the *S. aureus* group, we quantified the color of the GgC nonwoven mats by using the CMYK color model, which gives chrominance values for cyan, magenta, yellow, and black, respectively. For a bacterial colony count greater than 1980, the chrominance values of yellow and black in the CMYK color model were greater than 80 and 50, respectively, which caused the GgC nonwoven mats to take on a brown to dark brown color. In contrast, when the bacteria count was falling in 990–1980, the chrominance values of black and yellow in the CMYK color model both decreased to 40–43 and 19–42, resulting in a light brown color. Furthermore, when the bacterial count was below 990, the chrominance values of

Fig. 2 Categories of color indicator behavior of the GgC nonwoven mats upon indirect contact with varying counts of *S. aureus* and *E. coli*. The numbers in parentheses give the chrominance values for cyan, magenta, yellow, and black, respectively, based on the CMYK color model.

yellow and black in the CMYK color model were less than 20 and 40, respectively, resulting in a mostly white to grey color for the GgC nonwoven mats. Thus, the color of the GgC nonwoven mats showed a strong relationship associated with the amount of *S. aureus*, a Gram-positive bacteria, in the surrounding environment.

To further probe this relationship between the bacterial count and the color of the GgC nonwoven mats, we repeated our

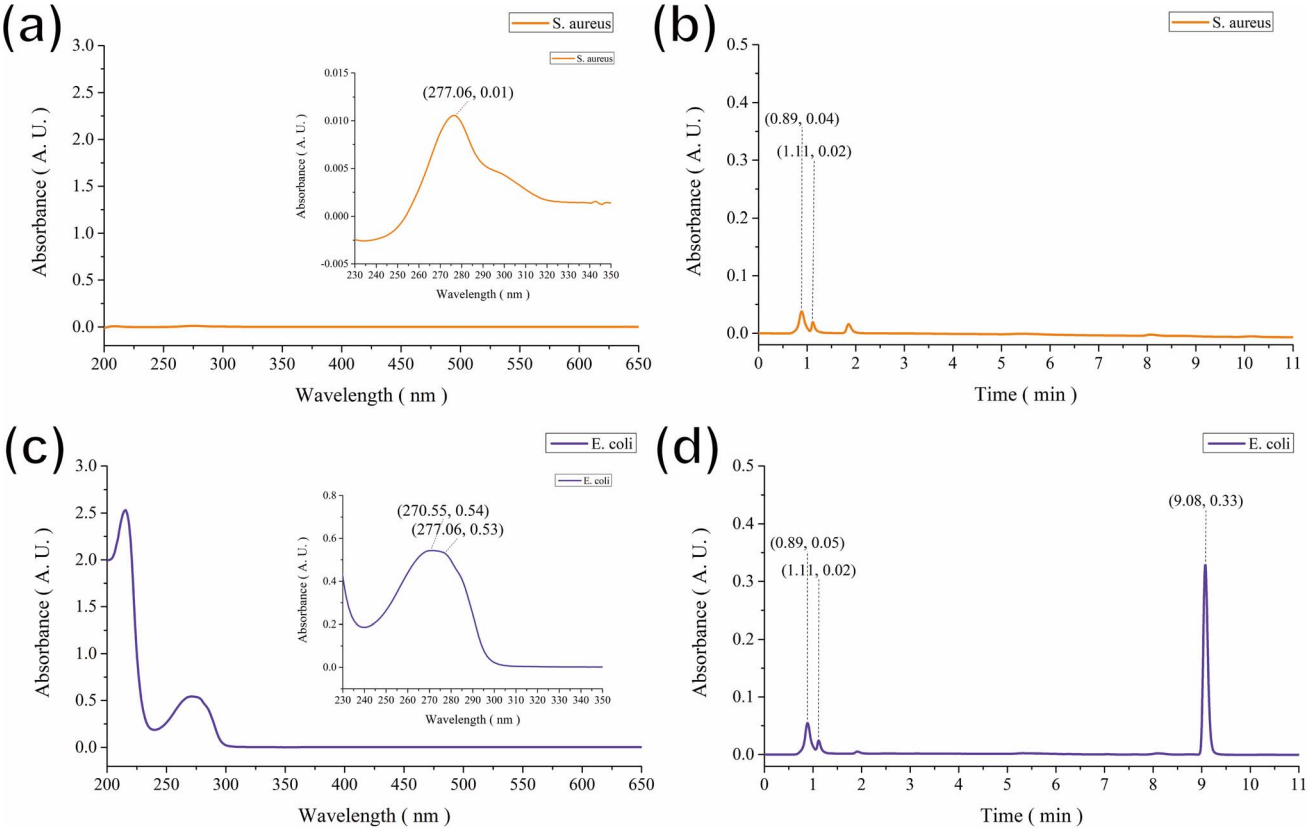

Fig. 3 HPLC spectra of (a and b) *S. aureus* and (c and d) *E. coli*.

investigation with *E. coli*, a Gram-negative bacteria. For the *E. coli* group, we applied the same CMYK color model to quantitatively determine the color of the GgC nonwoven mats. For bacteria counts exceeding 2000, the chrominance values for yellow and black in the CMYK color model were greater than 80 and 70, respectively, causing the nonwoven mat to take on a dark brown color. However, when the bacteria count was 952–1360, the chrominance values for yellow and black in the CMYK color model decreased to 29–44. When the bacteria count was less than 900, the chrominance values for yellow and black remained at approximately 11–29.

Thus, the color of the GgC nonwoven mats can be used as an indicator to monitor the counts of bacteria in the surrounding air. Overall, the yellow and black color components of the GgC nonwoven mats showed a strong positive relationship with the bacteria count: dark brown (chrominance >80, count >2000), yellow (chrominance 10–44, count >1000–2000), and grey (chrominance <30, count <1000).

3.3 Plausible mechanism of the pathogen indication ability of GgC nonwoven mats

Based on the above observations, we hypothesized that the brown color displayed on the GgC nonwoven mats was the result of indirect contact between vaporized bacterial excretion contents above the agar plate and gallic acid in the nonwoven mat. To identify the key components generated during the bacterial culture that might react with gallic acid, the vapor was condensed by dry ice, and the condensed aqueous solution was analyzed by HPLC. As shown in Fig. 3, the primary peaks of *S. aureus* and *E. coli* bacteria were separated from those of the condensed fluids, with elution peaks appearing at retention times of 0.89 and 1.11 min for *S. aureus* and 9.08 min for *E. coli* (Fig. 3(b) and (d)). By analyzing the main peak spectra, we determined that the maximum absorbance wavelength was 277 nm for both *S. aureus* and *E. coli*, as shown in Fig. 3(a) and (c), although there was a broad shoulder band at approximately 270 nm corresponding to the condensed fluid from *E. coli*, as shown in Fig. 3(c). According to previous reports, the elution bands at 1.40 min and 9.11 min most likely correspond to laccase[23,24] or various amino acids[25] that could result from bacterial exo-metabolism. Therefore, we hypothesized that the contents of the harvested condensed fluids might contain laccase or various amino acids in the vapor of the agar plates and that the gallic acid in the GgC nonwoven mats produced a brown color upon enzymatic or non-enzymaticreaction.

Laccase is a multicopper oxidase produced by plants, fungi, insects, and bacteria[26] that catalyzes the oxidation of a variety of phenolic compounds resulting from the generation of unstable radicals.[27] Laccase has been used in the biosynthesis of melanin pigments, biofuel production, wine clarification, biosensor development, and lignan removal.[28,29] However, applications of laccase are hindered by low productivity and high production

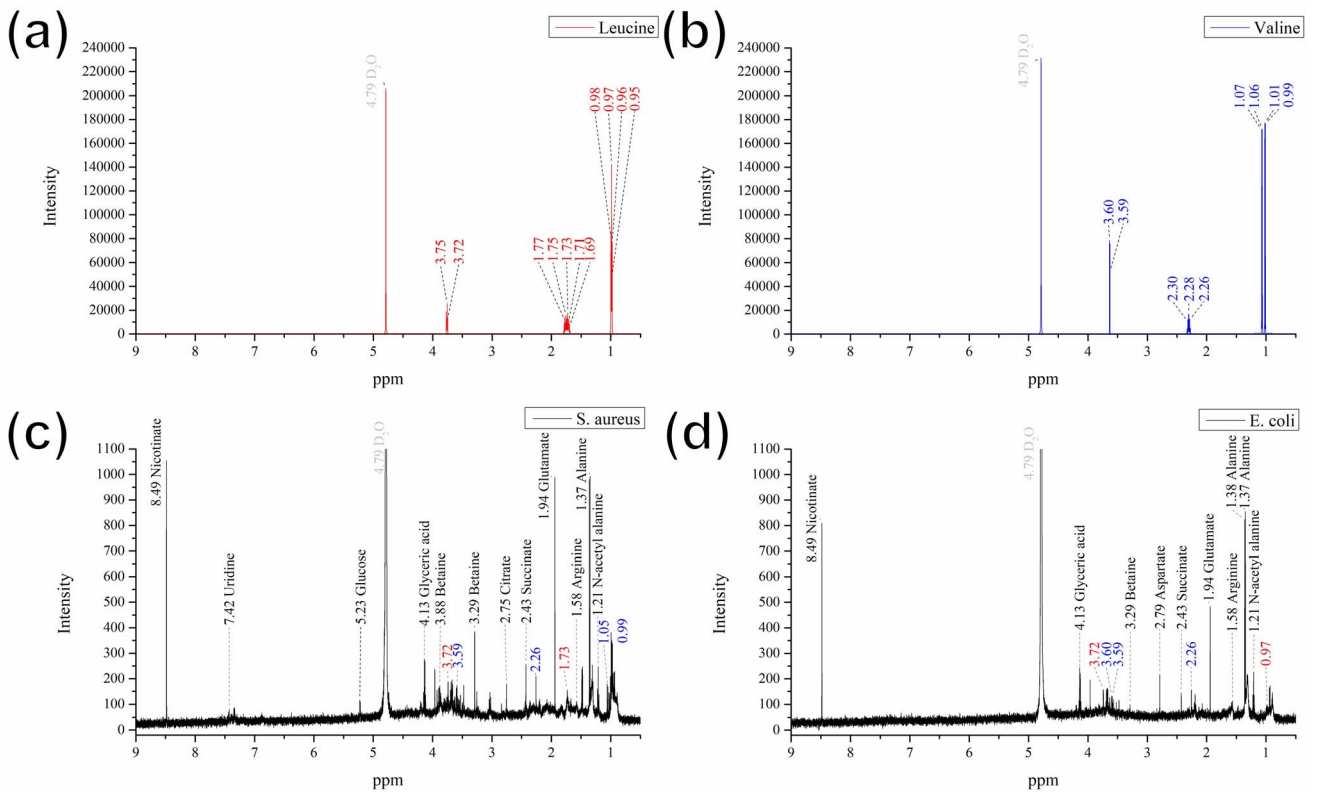

Fig. 4 NMR spectra of (a) leucine, (b) valine, (c) *S. aureus*, and (d) *E. coli*.

costs.[30] Amino acids are the basic units of protein, containing an amino group and a carboxylic group.[31] Although over 500 amino acids exist in nature, the amino acids primarily utilized in research are alpha-amino acids, which are used to form proteins.[32] Some necessary amino acids cannot be synthesized by the body and thus must be acquired through diet;[33] these essential amino acids include histidine, isoleucine, leucine, lysine, methionine, phenylalanine, threonine, tryptophan, and valine.[34]

Some of previous studies have analyzed amino acid biosynthesis and metabolic changes *via* NMR spectroscopy of *E. coli* extracts.[35] Thus, to investigate the plausible mechanism governing the color change observed in the GgC nonwoven mats upon exposure to bacteria, we analyzed the contents of the condensed fluids by NMR (Fig. 4). By comparing our NMR spectra with results in the literature,[23–25] we found that most of the prominent peaks in the spectra for the *S. aureus* and *E. coli* condensed fluids could be attributed to various amino acids (see Fig. 4(c) and (d)), such as, lysine, alanine, glycine, glutamate, succinate, aspartate, and *n*-acetyl alanine, except. Therefore, we compared our spectrum with some other amino acids and found that the NMR peaks at 0.99, 1.06, and 2.26 ppm could be attributed to the standard compound valine (Fig. 4(b), shown in blue). The remaining peaks at 0.97, 1.73, and 3.72 ppm could be attributed to the standard compound leucine (Fig. 4(a), shown in red). As shown in Fig. 4(c) and (d), the most prominent peaks for the *S. aureus* and *E. coli* condensed fluids occurred at 1.37 ppm, 1.94 ppm, and 8.49 ppm, which could be designated as alanine, glutamate, and nicotinate contribution, based on literature by Palama *et al.* and coworkers.[25] Also, the discrepant peak in the NMR spectrum acquired from the *E. coli* condensed fluid was identified at 2.79 ppm, which could be interpreted as a aspartate contribution, based on research by Palama *et al.*[25]

Based on the above evidence, we can preliminarily attribute the elution bands at 0.89 min, 1.11 min, and 9.08 min in the HPLC results (Fig. 3) to glutamate, aspartate, or the amino acids valine and leucine. We confirmed these preliminary assignments by HPLC analysis and comparison with that of using standard compounds of glutamate, aspartate, valine, and leucine for comparison (see Fig. S1† for comparison). In summary, we determined that the major influential components in the vapor generated during bacterial culture are glutamate, aspartate, and the amino acids valine and leucine. These crucial components react with the GgC nonwoven mats, causing the color to change.

To determine the mechanism of the color change observed in the GgC nonwoven mats, we applied FTIR spectroscopy to characterize the surface chemical structure for both GgC and GC nonwoven mats. The absorption bands of amide A, amide I, and amide II in the GC mat occur at 3297 cm^{-1} (N–H stretching), 1637 cm^{-1} (C=O), and 1541 cm^{-1} (N–H in-plane scissoring), respectively. When gallic acid was crosslinked with gelatin, the amide A and amide II bands showed a red shift from 3297 cm^{-1} to 3284 cm^{-1} and from 1541 cm^{-1} to 1535 cm^{-1},

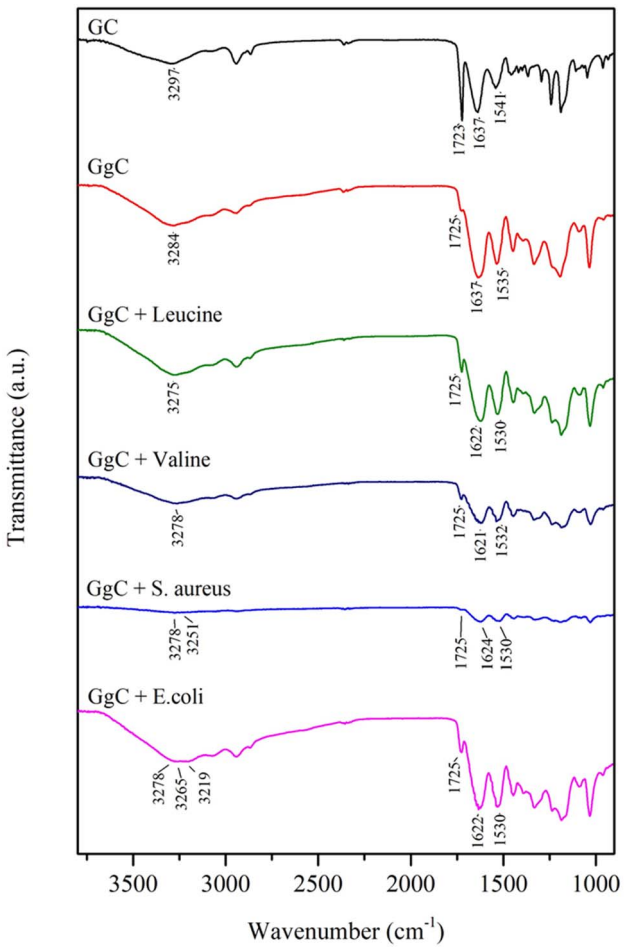

Fig. 5 FTIR results for GC, GgC, leucine, valine, *S. aureus*, and *E. coli*.

whereas the amide I band remained unchanged in the GgC mat (Fig. 5). This result reveals that the addition of gallic acid can bind with the N–H bond of the gelatin molecule *via* hydrogen bonding as gallic acid bears lots of hydroxyl and carboxylic acid functional groups.

When amino acids react with gallic acid, the red shift of the amide A, amide I, and amide II bands indicates the mechanism of how the essential amino acids possibly influence the GgC nonwoven mat. The absorption bands at 3284 cm^{-1} and 1637 cm^{-1} shift to lower frequencies when GgC reacts with leucine or valine. The peak at 3284 cm^{-1} shifted to 3275 cm^{-1} (leucine) or 3278 cm^{-1} (valine), potentially indicating that the hydrogen bonding of between gallic acid and gelatin reduced the stretching frequency. It is worth of noting that the amide I band showed a red shift (from 1637 cm^{-1} to 1621–1622 cm^{-1}) caused by reduction/oxidation. When the vapor from the agar plates entrains amino acids to the attached GgC nonwoven mats, leucine or valine molecules may oxidize the gallic acid to a type of quinone derivative and the amino acid itself was reduced to alkanol amine. This reduction can then reduce the amide I stretching band from approximately 1637 cm^{-1} to 1621–1622 cm^{-1}.

Various amino acids were present in the *S. aureus* and *E. coli* condensed fluids, as demonstrated by HPLC and NMR results. When GgC nonwoven mats adsorbed the vapor from the agar plates, amino acids bonded with the gallic acid to generate the plural red shift from 3284 cm^{-1} to 3278 cm^{-1}, 3251 cm^{-1}, 3265 cm^{-1}, and 3219 cm^{-1}, as shown in Fig. 5. The proposed mechanism governing the indication ability of our GgC nonwoven mats is illustrated in Scheme 2.

The proposed mechanism of this color change can be summarized as follows. The vapor from the agar plates brings amino acids excreted by the bacteria into contact with the GgC nonwoven mats. The amino acids then act as a oxidizing agent to oxidize the gallic acid, potentially at its hydroxyl group sites. When the reduction/oxidation reaction occurs between the amino acids and gallic acid, the amino acids are reduced to alkanol amine, and the gallic acid is oxidized to quinone, as shown in Scheme 2. The production of quinone causes the absorption bands of OH and C=C to shift to 3265 cm^{-1} and 1621 cm^{-1}, respectively. The conjugated system of quinone shifts the absorption closer to 400 nm,[16] resulting in a complementary color (yellow brown). The redox reaction changes both the molecular structure and optical properties of the gallic acid. Moreover, the accumulation of quinone byproduct increases with an increasing level of amino acids as the bacteria count rises. For a bacteria count greater than 2000, the generated quinone byproduct was sufficiently abundant to shift the absorption wavelength to the range of visible light, causing the yellow chrominance value in the CMYK color model to exceed 80.

3.4 *In vitro* antipathogenic activity test

To probe the antibacterial activity and time-kill curve assay of the GgC nonwoven mats, we dissolved the mats in LB broth medium. GgC solutions of 10 000 ppm and 20 000 ppm exhibited 81% and 97% sterilization efficiency against *S. aureus* and *E. coli*, respectively (Fig. 6(a) and (b)). As shown in Fig. 6(c) and (d), the distinct reductions of the bacteria were observed after 24 h which were exposed to GgC solutions at concentrations of 10 000 ppm and 20 000 ppm. The results of the time-kill curve exhibited significant time-dependent action and the maximum reduction in viable counts was over 7×10^9 CFU mL^{-1} in 24 h for the GgC solutions of 20 000 ppm. These results demonstrate that the GgC nonwoven mat can serve as a chemical antibacterial agent against *S. aureus* and *E. coli*, in addition to its ability to physically intercept pathogens *via* its nonwoven mat filtration function. Another type of pathogens that is threatening to human is virus, such as covid-19 pandemic in the past three years. Therefore, we are inspired to test the antibacterial activity of the GgC nonwoven mats toward virus. To probe the antivirus activity of the GgC nonwoven mats, we dissolved the mats in the medium and applied plaque assay to detect the infection rate. In plaque therapy assay, the safe concentration (1000 ppm) that was identified through the MTT assay (Fig. S2†) was firstly tested. When the infected cells were incubated with GgC solution (1000 ppm), the gallic acid of GgC solution (1000 ppm) was not

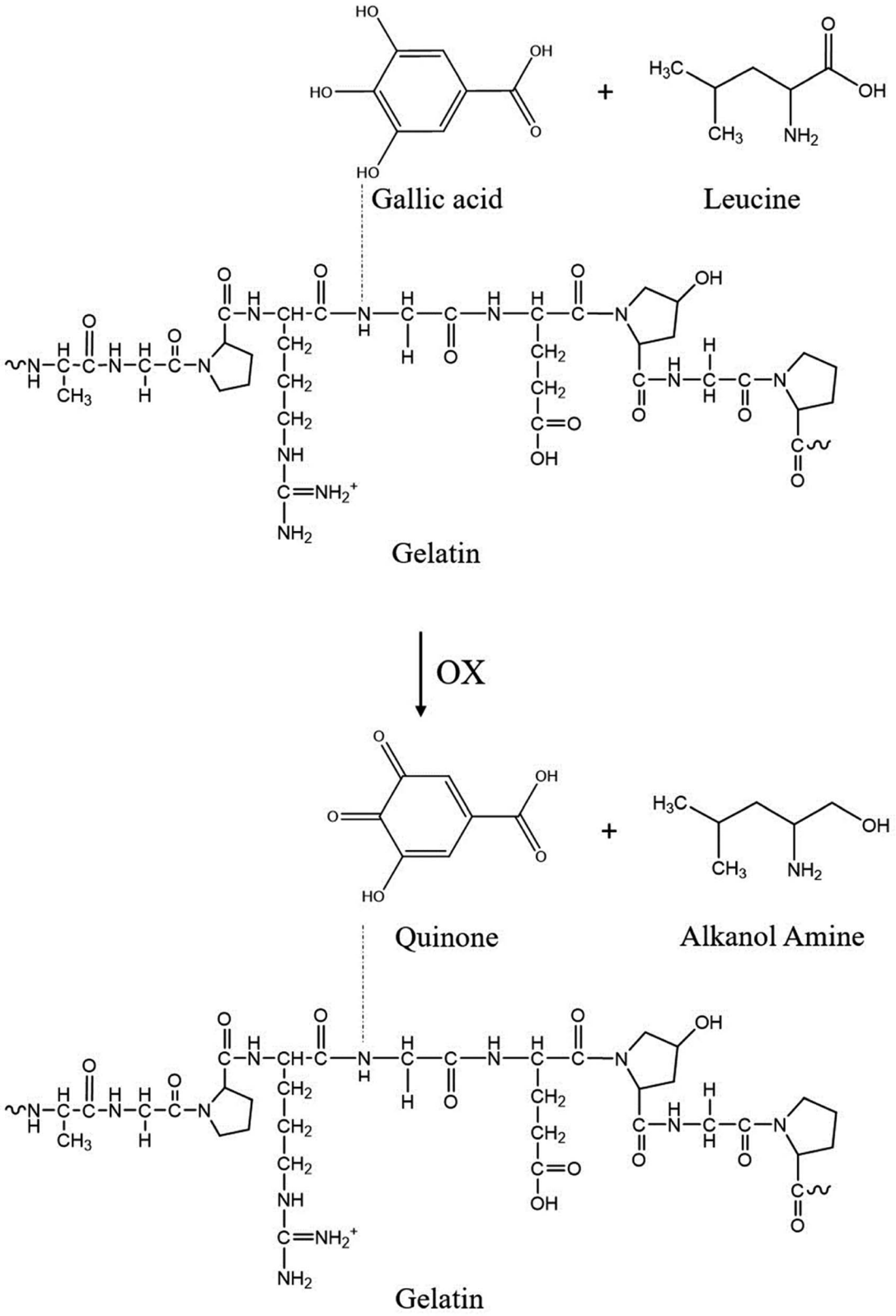

Scheme 2 Mechanism by which gallic acid indicates the level of bacteria in the surrounding environment.

enough to inhibit the H1N1 virus infection (Fig. 7(a)), thus virus plaque is still observed in cell plate. In plaque neutralization assay, In Fig. 7(b), H1N1 virus solution was reacted with high concentration of GgC solution (up to 40 000 ppm) before the infection of MDCK cells that could provide enough gallic acid to completely inhibit the H1N1 virus (see Fig. 7(b)) as no

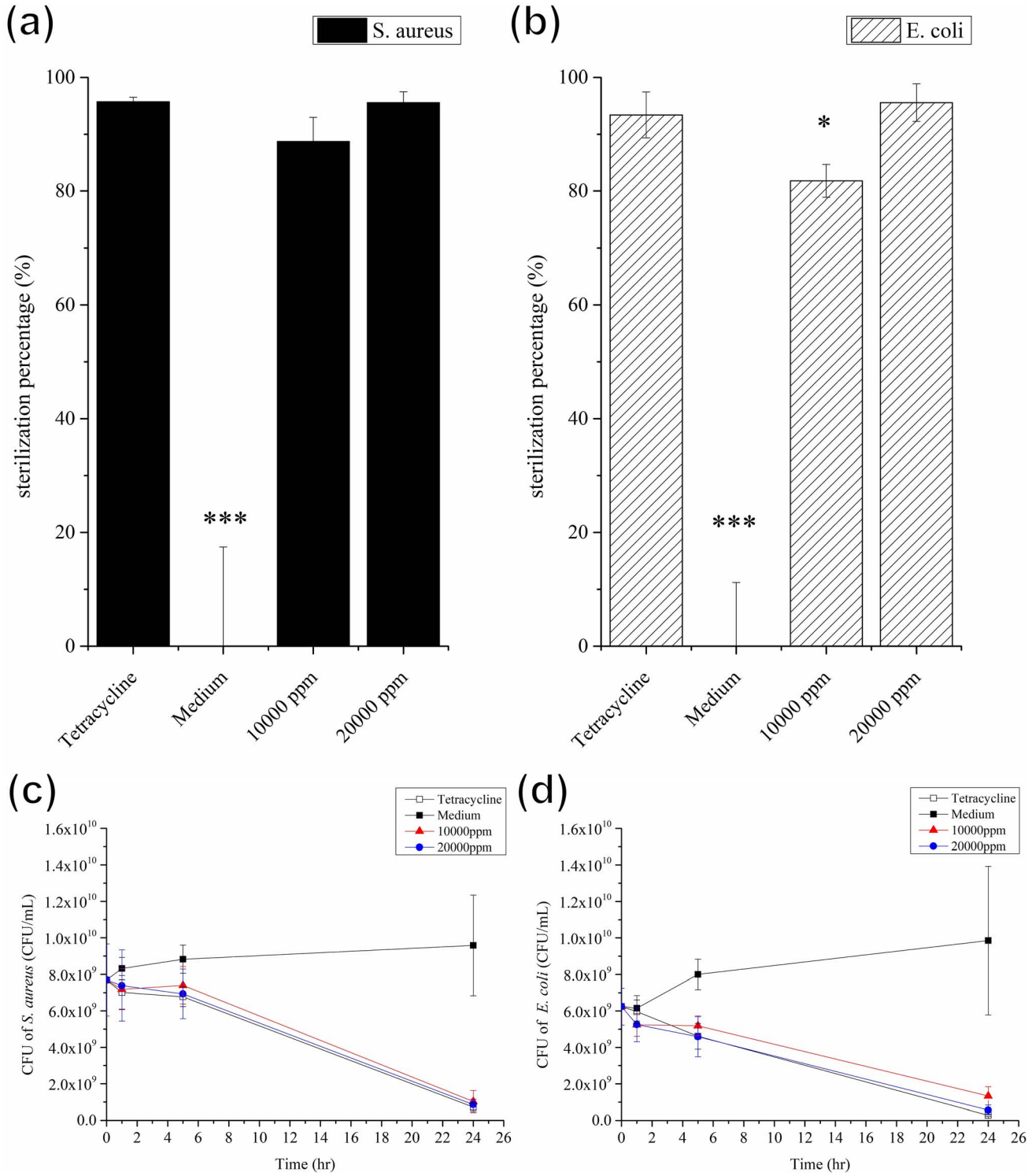

Fig. 6 Antibacterial effect and Time-kill curve assay of 10 000 ppm and 20 000 ppm GgC/medium against *S. aureus* (1.36×10^{10} CFU mL^{-1}) and *E. coli* (2.73×10^{9} CFU mL^{-1}). (a) Sterilization efficiency against *S. aureus*. (b) Sterilization efficiency against *E. coli*. (c) Time-kill curve assay against *S. aureus*. (d) Time-kill curve assay against *E. coli*. Error bars show the standard error of the mean. Significance was calculated by Student's *t*-test (*$p < 0.05$, **$p < 0.01$, ***$p < 0.001$).

virus plaque is observed. These results demonstrate that the antivirus activity of GgC nonwoven mat. Although the GgC nonwoven mat could not provide the therapy effect in safe concentration (1000 ppm), it still could be applied to prevent the virus infection in high concentration conditions when fabricating the biomaterial for protection.

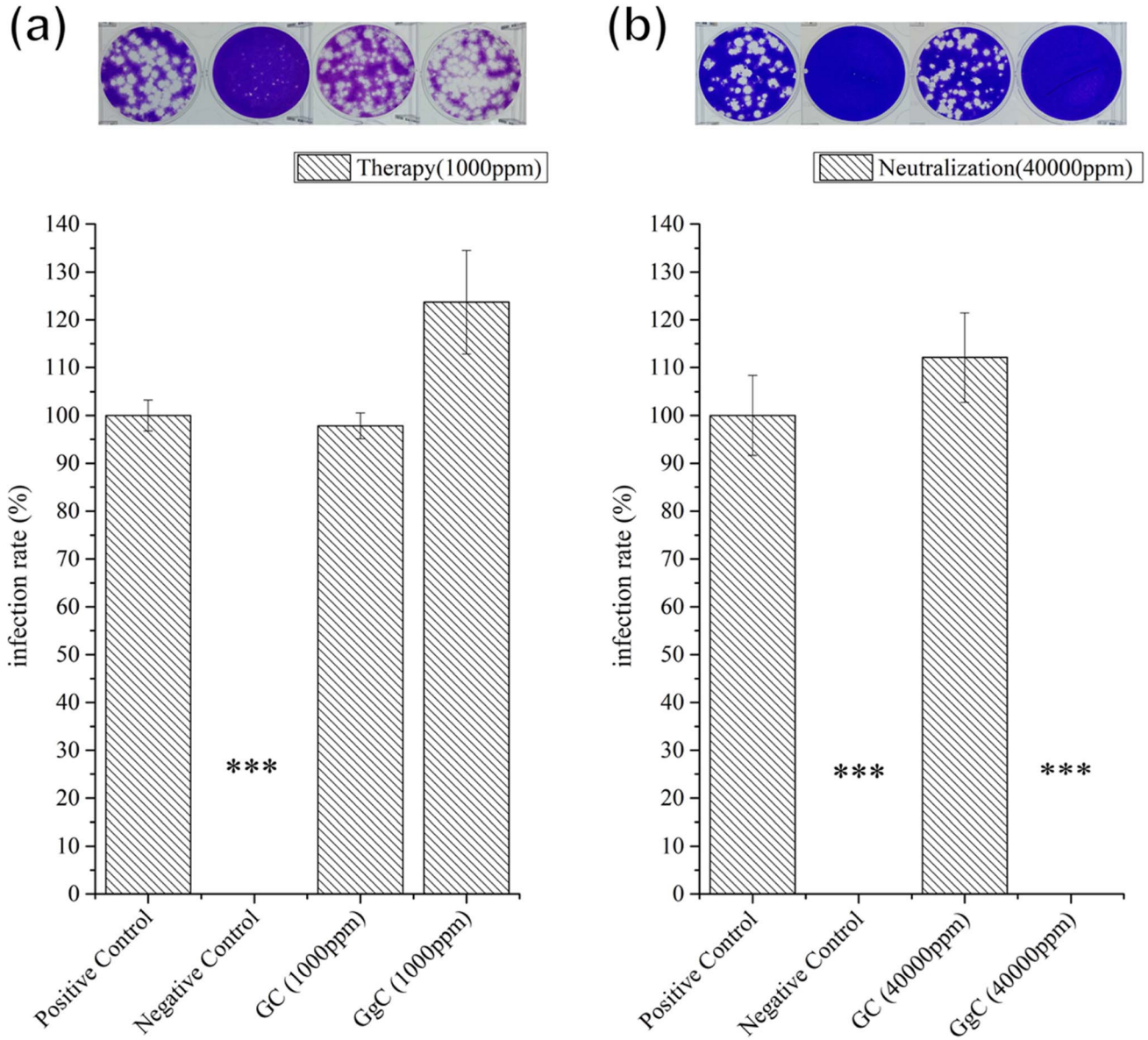

Fig. 7 Plaque assay of GC and GgC against H1N1. (a) Therapy assay (b) neutralization assay. Error bars show the standard error of the mean. Significance was calculated by Student's *t*-test (*$p < 0.05$, **$p < 0.01$, ***$p < 0.001$). Negative control: Tamiflu.

4. Conclusions

In this study, we successfully developed and fabricated GgC nonwoven mats composed of gelatin, gallic acid, and PCL, with the ability to intercept pathogens,indicate the bacteria count in the surrounding airborne environment and anti-pathogen abilities. We demonstrated that gallic acid serves a vital role in the GgC nonwoven mats by crosslinking gelatin and indicating the risk of airborne bacterial infection. As a crosslinking agent, gallic acid improves the physical structure of the electrospun fibers and produces a uniform distribution of pore size and porosity, which enables the GgC nonwoven mats to intercept bacteria or aerosol or particulate matter. Moreover, gallic acid causes the GgC nonwoven mats to change in color from white to brown upon indirect contact with bacteria.

We investigated a plausible mechanism for this color change behavior by analyzing the products excreted during bacterial culture. We identified several amino acid components, with glutamate, aspartate, valine, and leucine as the major components. When the amino acids from the bacteria come into contact with the GgC nonwoven mats, the gallic acid is oxidized to quinone, which shifts the UV-vis absorption wavelength to 400 nm. This change in visible color enables the mats to indicate the counts of bacteria in the surrounding environment. Although GgC nonwoven mats have been proven its plausible mechanism for indicating the colonies of *S. aureus* and *E. coli*, COVID-19-relevant experiments will be the next prominent target of our further study. However, the fatal virus-associated experiments must be entrusted to the level 4 laboratory which made the virus-associated results difficult to obtain and

conduct to avoid sharing the precious COVID-19 research resource at this emergency moment. Therefore, government and research institution experts suggest us giving priority to probe the antiviral activity of non-woven mats against H1N1 viruses firstly at this post-COVID-19 pandemic era. Although the GgC nonwoven mat could not provide the therapeutic efficacy in the range of safe concentration (1000 ppm), it still could be applied to prevent the virus infection in high concentration conditions when fabricating the biomaterial for protection and prevention of lethal infection, like H1N1 and COVID-19 infection. In summary, the GgC nonwoven mats presented herein could be applied to be an excellent and potential antibacterial material, a real-time indicator, which could be combined with dressing or filtration mask to indicate nearby bacteria colonies based on their color change behavior.

Conflicts of interest

There are no conflicts of interest to declare.

Acknowledgements

This work was supported by grants from the Ministry of Science and Technology, Taiwan (MOST 109-2221-E-011-036, 108-2221-E-011-113, and 111-2221-E-011-151).

References

1 J. D. Berman and K. Ebisu, Changes in US air pollution during the COVID-19 pandemic, *Sci. Total Environ.*, 2020, **739**, 139864.
2 S. Khan, *et al.*, Risk communication and community engagement during COVID-19, *Int. J. Disaster Risk Reduct.*, 2022, **74**, 102903.
3 S. Gautam, COVID-19: air pollution remains low as people stay at home, *Air Qual., Atmos. Health*, 2020, **13**, 853–857.
4 T. Amnuaylojaroen and N. Parasin, The association between COVID-19, air pollution, and climate change, *Front. Public Health*, 2021, **9**, 662499.
5 D. Rodríguez-Urrego and L. Rodríguez-Urrego, Air quality during the COVID-19: PM2. 5 analysis in the 50 most polluted capital cities in the world, *Environ. Pollut.*, 2020, **266**, 115042.
6 M.-Yi Bai, D.-T. Wang and J. Sin, Sericin-based wound dressing with wound moisture indicator, *Materialia*, 2018, **1**(9), 37–45.
7 M. Abid, *et al.*, Antioxidant properties and phenolic profile characterization by LC–MS/MS of selected Tunisian pomegranate peels, *J. Food Sci. Technol.*, 2017, **54**, 2890–2901.
8 M. Abbas, *et al.*, Natural polyphenols: An overview, *Int. J. Food Prop.*, 2017, **20**(8), 1689–1699.
9 Y. Zhang, *et al.*, Gallic acid liposomes decorated with lactoferrin: Characterization, *in vitro* digestion and antibacterial activity, *Food Chem.*, 2019, **293**, 315–322.
10 L. Guo, *et al.*, Purification and characterization of hydrolysable tannins extracted from Coriaria nepalensis bark using macroporous resin and their application in gallic acid production, *Ind. Crops Prod.*, 2021, **162**, 113302.
11 B. Badhani, N. Sharma and R. Kakkar, Gallic acid: A versatile antioxidant with promising therapeutic and industrial applications, *RSC Adv.*, 2015, **5**(35), 27540–27557.
12 K. Nakamura, *et al.*, Bactericidal action of photoirradiated gallic acid *via* reactive oxygen species formation, *J. Agric. Food Chem.*, 2012, **60**(40), 10048–10054.
13 K. Limpisophon and G. Schleining, Use of gallic acid to enhance the antioxidant and mechanical properties of active fish gelatin film, *J. Food Sci.*, 2017, **82**(1), 80–89.
14 L. Wang, L. Lin and J. Pang, A novel glucomannan incorporated functionalized carbon nanotube films: Synthesis, characterization and antimicrobial activity, *Carbohydr. Polym.*, 2020, **245**, 116619.
15 C. Pu, *et al.*, Resveratrol-loaded hollow kafirin nanoparticles *via* gallic acid crosslinking: An evaluation compared with their solid and non-crosslinked counterparts, *Food Res. Int.*, 2020, **135**, 109308.
16 L. Guo, *et al.*, Biodegradable anti-ultraviolet film from modified gallic acid cross-linked gelatin, *ACS Sustain. Chem. Eng.*, 2021, **9**(25), 8393–8401.
17 W.-P. Chuang and B.-C. Hsieh, Development of a gallic acid based time temperature indicator with adjustable activation energy, *Food Control*, 2023, **144**, 109396.
18 Y. Zhang, *et al.*, Electrospinning of gelatin fibers and gelatin/PCL composite fibrous scaffolds, *J. Biomed. Mater. Res., Part B*, 2005, 156–165.
19 M. Li, *et al.*, Transplacental transfer efficiency of maternal antibodies against influenza A (H1N1) pdm09 virus and dynamics of naturally acquired antibodies in Chinese children: a longitudinal, paired mother–neonate cohort study, *Lancet Microbe*, 2023, DOI: **10.1016/S2666-5247(23)00181-7**.
20 K. Yue, *et al.*, Structural analysis of photocrosslinkable methacryloyl-modified protein derivatives, *Biomaterials*, 2017, **139**, 163–171.
21 K. Yue, *et al.*, Structural analysis of photocrosslinkable methacryloyl-modified protein derivatives, *Biomaterials*, 2017, **139**, 163–171.
22 M. J. Mochane, *et al.*, Morphology and properties of electrospun PCL and its composites for medical applications: A mini review, *Appl. Sci.*, 2019, **9**(11), 2205.
23 P. S. Chauhan, B. Goradia and A. Saxena, Bacterial laccase: recent update on production, properties and industrial applications, *3 Biotech*, 2017, **7**(5), 323.
24 T. C. Ezike, *et al.*, Substrate specificity of a new laccase from Trametes polyzona WRF03, *Heliyon*, 2021, **7**(1), e06080.
25 T. L. Palama, *et al.*, Identification of bacterial species by untargeted NMR spectroscopy of the exo-metabolome, *Analyst*, 2016, **141**(15), 4558–4561.
26 F. Wang, *et al.*, Enhanced laccase production by Trametes versicolor using corn steep liquor as both nitrogen source and inducer, *Bioresour. Technol.*, 2014, **166**, 602–605.
27 E. Marco-Urrea, and C. A. Reddy, Degradation of chloro-organic pollutants by white rot fungi, *Microbial degradation of xenobiotics*, 2012, pp. 31–66.

28 U. N. Dwivedi, *et al.*, Structure–function relationship among bacterial, fungal and plant laccases, *J. Mol. Catal. B: Enzym.*, 2011, **68**(2), 117–128.
29 A. E. Adekunle, *et al.*, Laccase production from Trametes versicolor in solid-state fermentation of steam-exploded pretreated cornstalk, *Waste Biomass Valorization*, 2017, **8**, 153–159.
30 J. F. Osma, J. L. Toca-Herrera and S. Rodríguez-Couto, Cost analysis in laccase production, *J. Environ. Manage.*, 2011, **92**(11), 2907–2912.
31 M. Akram, *et al.*, Amino acids: A review article, *J. Med. Plants Res.*, 2011, **5**(17), 3997–4000.
32 G. Wu, Amino acids: metabolism, functions, and nutrition, *Amino Acids*, 2009, **37**, 1–17.
33 M. C. Aristoy, and F. Toldrá, Essential amino acids, *Handbook of seafood and seafood products analysis*, CRC Press, 2009, pp. 305–326.
34 M. J. Lopez, and S. S. Mohiuddin, *Biochemistry, essential amino acids*, 2020.
35 Q. Liu, *et al.*, Evaluation of the metabolic response of Escherichia coli to electrolysed water by 1H NMR spectroscopy, *LWT–Food Sci. Technol.*, 2017, **79**, 428–436.